

Supporting Information

Surface Asymmetry of Coated Spherical Nanoparticles

*Amelie H.R. Koch,[†] Gaëtan Lévêque,[‡] Sebastian Harms,[§] Karmena I. Jaskiewicz,[†] Max
Bernhardt,[†] Andreas Henkel,[§] Carsten Sönnichsen,[§] Katharina Landfester,[†] George Fytas^{*,†,#}*

[†]Max Planck Institute for Polymer Research, Ackermannweg 10, 55128 Mainz, Germany

[‡]Institut d'Électronique, de Microélectronique et de Nanotechnologie (IEMN), UMR-CNRS
8520, UFR de Physique, Université de Lille 1, 59655 Villeneuve d'Ascq, France

[§]Institut für Physikalische Chemie, Johannes Gutenberg Universität, Duesbergweg 10-14, 55128
Mainz, Germany

[#]Department of Materials Science, University of Crete and IESL/FORTH, 71110 Heraklion,
Greece

Corresponding Author

*Email: fyta@mpip-mainz.mpg.de

S1. Preparation of functionalized gold nanospheres

A stock of gold spheres was synthesized according to a literature procedure.¹ SH-PEG-OCH₃ (M_w = 736 Da, M_w = 2015 Da, M_w = 5079 Da), SH-PEG-COOH (M_w = 4975 Da), Cetyltrimethylammonium bromide (CTAB), Mercapto undecanoic acid (MUA) and DNA (T10: Thymine 10-mer with 5'-Thiolink-C6. T40: Thymine 40-mer with 5'-Biotin-C6. Both purchased from Biomers.net), were bound to the particles by overnight incubation at room temperature as described by Hanauer et al.²

S2. Single particle Polarisation Anisotropy (PA) measurements

PA measurements were carried out at an optical microscopy system which is based on a motorized inverted microscope equipped with a piezo scanning stage, a z-piezo, a spectroscopy system, and an autosampler. We use self-made flow cells composed of two microscope cover slips. All components are controlled by a central MATLAB based software. A spectral precision for the plasmon peak of 0.3 nm is achieved by refining the exact nanoparticle position before each measurement. The polarization dependency was investigated by inserting a polarization filter in the detection light path. The spectra were acquired every 15° angle from 0° to 180°.

S3. Transmission Electron Microscopy (TEM)

5 µL of the aqueous solutions of Gold-NPs were deposited on a 300-mesh copper grid with a coal film. The samples were dried in air. (HighResolution-)TEM images were obtained on a FEI Tecnai F20 at 200 kV.

S4. UV-Vis Spectroscopy

All UV-Vis measurements were recorded on a PerkinElmer LAMBDA 25 UV-Vis spectrometer, using water as a reference.

S5. Photon correlation spectroscopy (PCS)

The normalized light scattering intensity $I(q,t)$ autocorrelation function $G(q,t) \equiv \langle I(q,t)I(q) \rangle / I(q)^2$ was recorded over a broad time range (10^{-7} – 10^3 s) at different scattering wave vectors q with an ALV/LSE-5004 goniometer/correlator setup using lasers with two different wavelengths $\lambda = 632$ nm (HeNe laser) and $\lambda = 532$ nm (Compass 215M, Coherent, Santa Clara, CA). The scattering vector $\mathbf{q} = \mathbf{k}_s - \mathbf{k}_i$ with k_s and k_i being the wave vectors of the scattered and incident light, respectively, has magnitude $q = (4\pi n/\lambda)\sin(\theta/2)$ (n and θ are the solution refractive index and the scattering angle, respectively). We have performed both polarized (VV) and depolarized (VH) PCS experiments using a vertically (V) polarized incident laser beam and selected the scattered light polarized vertically (VV-configuration) and horizontally (VH-configuration) to the scattered plane (k_i, k_f) . The measurements were carried out at temperature $T = 20^\circ\text{C}$. Only for Au-citrate and Au-PEG₁₆, PCS was performed also at 50°C .

For spherical NPs, the translational diffusion coefficient D^t is directly obtained from the diffusive relaxation rate $\Gamma = \Gamma_{VV} = D^t q^2$ of the isotropic relaxation function. For this case, no scattering in VH can be observed. For anisotropic particles, rotational motion is unequal to the translational motion and can be observed in VH geometry. D^r is the rotational diffusion coefficient and $\Gamma_{VH} = 6D^r + D^t q^2$. The isotropic and anisotropic relaxation functions are:

$$C_{VH}(q,t) = \exp[-\Gamma_f t] \quad (S3a)$$

$$C_{VV}(q,t) = a_f \exp[-\Gamma_f t] + a_s \exp[-\Gamma_s t] \quad (S3b)$$

where $\Gamma(q)$ is the relaxation time for the fast (f) and slow (s) processes, respectively. The VV scattering includes both isotropic and anisotropic contributions and therefore C_{VV} becomes bimodal, with fast and slow processes characterized by amplitudes a_f and $a_s = (1 - a_f)$ and rates Γ_f and Γ_s .

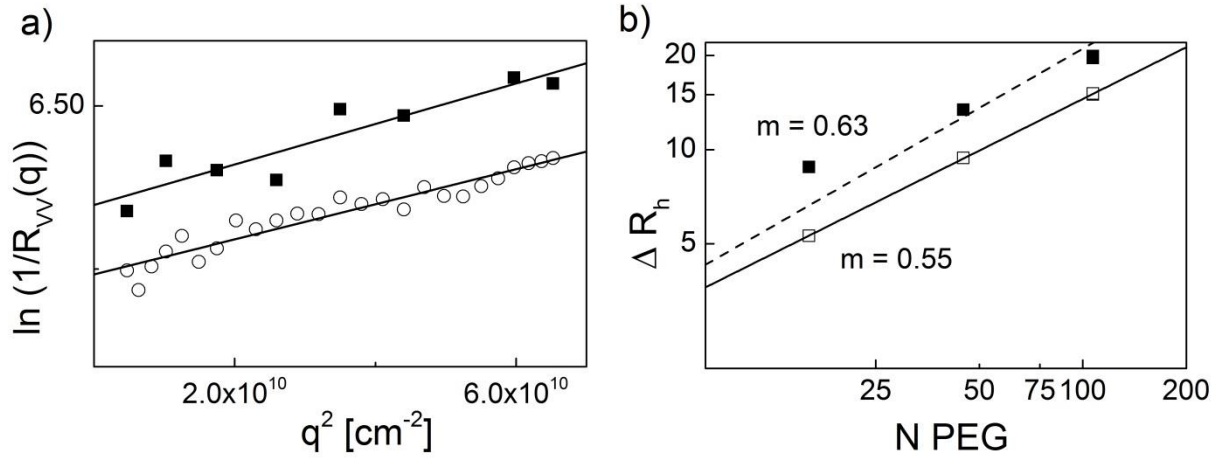


Figure S1. a) Guinier plot, $\ln[1/R_{VV}(q)]$ vs q^2 , for either the total polarized $R_{VV}(q)$ (open circles) or the pure isotropic $R_{ISO}(q)$ (solid squares) contribution obtained from the relaxation function $C_{VV}(q,t)$. b) Grafted layer thickness plot vs. degree of polymerization of the PEG grafts for AuNP with $d = 44$ nm in a log-log presentation yielding a slope $\nu=0.55$ and $\nu=0.63$ below and above the scaling (~ 0.588) exponent for good solvency.

Table S1. Characteristic dimensions of grafted Au nanospheres with diameter of 41 nm, depolarization ratio at two optical wavelengths and the plasmon resonance wavelength.

	R_h [nm]	R_r [nm]	$\rho = R_{VH}/R_{VV}$		λ_{max} [nm]
			632nm	532nm	
Au-citrate	23.5 ± 0.7	36.3 ± 0.5	0.12	0.02	522
Au-PEG₁₆	23.0 ± 0.7	31.0 ± 1.5	0.01	0.01	523
Au-PEG₄₅	24.9 ± 0.7	29.5 ± 0.7	0.01	0.01	524
Au-PEG₁₀₇	30.4 ± 0.6	37.6 ± 0.7	0.01	0.01	524
Au-PEG_{107-COOH}	31.9 ± 0.3	34.7 ± 0.7	0.01	0.01	523
Au-CTAB	22.8 ± 0.7	32.7 ± 0.3	0.04	0.01	525
Au-MUA	28.4 ± 0.5	36.6 ± 0.4	0.07	0.02	525

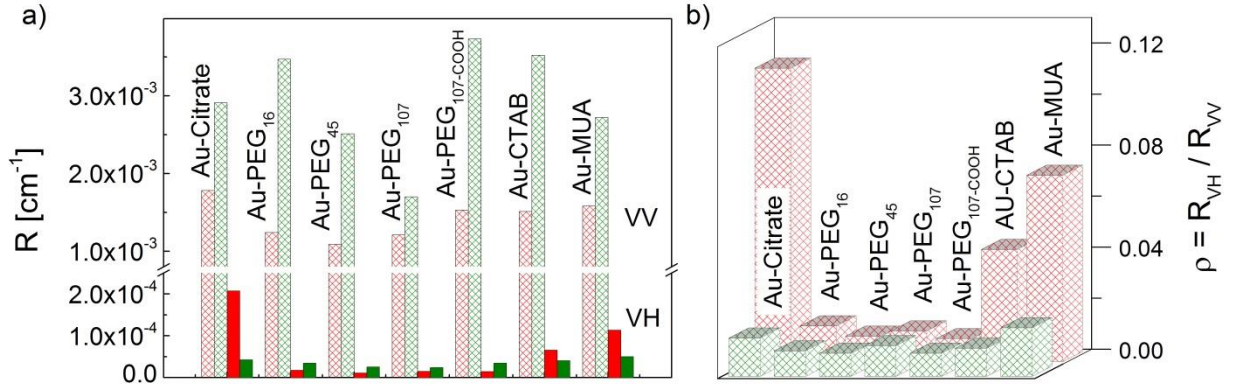


Figure S2. a) Absolute Rayleigh ratio for polarized (R_{VV} , hatched areas) and depolarized (R_{VH} , solid areas) light scattering and b) depolarization ratio ρ at 532 nm (green) and 632 nm (red) for a dilute suspension of Au nanospheres with 41 nm diameter core and different grafts as indicated in the plots.

S6. Depolarization ratio of naked AuNPs with Green's tensor simulations

The effect of size dispersion on bared Au NPs has been investigated using the Green's tensor formalism,³ which allows computing the electromagnetic field scattered by a small object embedded in a multilayered environment, under an arbitrary monochromatic illumination of pulsation ω . It relies on the resolution of the Lippmann-Schwinger equation:

$$\mathbf{E} = \mathbf{E}_0 + k_0^2 \int_V \mathbf{G}_0(\mathbf{r}, \mathbf{r}', \omega) \overline{\overline{\Delta\epsilon}}(\omega) \mathbf{E}(\mathbf{r}', \omega) dV$$

where V is the NP's volume, \mathbf{E}_0 the complex incident electric field, \mathbf{E} the complex total electric field, and $k_0 = \omega/c$ is the wavevector of the light in the vacuum. The tensor $\mathbf{G}_0(\mathbf{r}, \mathbf{r}', \omega)$ is the Green's function of the homogeneous water environment, which is analytical for every couple $(\mathbf{r}, \mathbf{r}')$ in the whole space. Moreover, the tensor $\overline{\overline{\Delta\epsilon}}(\omega)$ is defined by:

$$\overline{\overline{\Delta\epsilon}}(\omega) = \overline{\overline{\epsilon}}(\omega) - \epsilon_B$$

where ϵ_B is the dielectric constant of water, and $\overline{\overline{\epsilon}}(\omega)$ is the gold dielectric constant, tensorial if the particle is polycrystalline, as explained earlier.

The first step of the simulation is the discretization of the Au NP in small polarizable cells, which allows accessing the NP internal field in every discretization point by numerically solving the Lippmann-Schwinger equation. The second step is the computation of the electric field scattered at infinity in the plane perpendicular to the incidence plane of the incident plane wave, through:

$$\mathbf{E}_s = k_0^2 \int_V \mathbf{G}_\infty(\theta, \phi; \mathbf{r}', \omega) \overline{\overline{\Delta\epsilon}}(\omega) \mathbf{E}(\mathbf{r}', \omega) dV$$

where (θ, ϕ) are the detection directions and $\mathbf{G}_\infty(\theta, \phi; \mathbf{r}', \omega)$ is the asymptotic Green's function.

Then, the polarized $I_{vv}^{\theta, \phi}$ and depolarized $I_{vh}^{\theta, \phi}$ intensities in the (θ, ϕ) direction are:

$$I_{vv}^{\theta, \phi} = \left| \mathbf{E}_s(\theta, \phi) \cdot \frac{\mathbf{E}_0}{\|\mathbf{E}_0\|} \right|^2, I_{vh}^{\theta, \phi} = |\mathbf{E}_s(\theta, \phi)|^2 - I_{vv}^{\theta, \phi}$$

Finally, the scattered intensities are numerically averaged on the incident field orientation in order to obtain $\rho(\omega) = I_{vh}(\omega)/I_{vv}(\omega)$.

S7. Theoretical model for the AuNPs polycrystallinity

A basic phenomenological model for the gold polycrystallinity has been implemented in the theoretical calculations. In this very simple approach, the polycrystalline particle is described as a spheroidal particle cut into several parallel slices of equal thickness l , along the direction of one of the principal axis, as shown in Fig. S3. When the particle is cut in 2, 3, 4, ..., n parts (n being called in the following the polycrystallinity order), l takes the values $2R/2, 2R/3, 2R/4, \dots, 2R/n$. Each interface between two slices behaves as a barrier that increases the collisions rate of electrons moving normally to it, due to the shortening of the electrons mean free path in that direction. For electrons moving parallel to the cut planes, the absorption rate can as well be increased due to a shortening of the mean-free path by the NP outer surface, when its diameter becomes smaller than the bulk free electron mean free path. This effect can be taken into account in the gold dielectric constant by increasing the absorption rate of the free-electrons contribution to ϵ_{bulk} , the dielectric constant of the bulk gold. Such corrections are usually applied to describe

the dielectric constant of gold NP of very small diameter, typically 20 nm and below.⁴ In this model, the dielectric constant reads:

$$\epsilon_l(\omega) = \epsilon_{bulk}(\omega) - \delta\epsilon_f(\omega) + \delta\epsilon_f^c(\omega)$$

where $\delta\epsilon_f(\omega)$ is the bulk contribution of the free electrons:

$$\delta\epsilon_f(\omega) = 1 - \frac{\omega_p^2}{\omega(\omega + i\Gamma)}$$

and $\delta\epsilon_f^c(\omega)$ is the corrected contribution of the free electrons:

$$\delta\epsilon_f^c(\omega) = 1 - \frac{\omega_p^2}{\omega(\omega + i\tilde{\Gamma})}, \quad \text{with:} \quad \tilde{\Gamma} = \Gamma + \frac{A}{L}$$

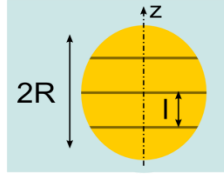


Figure S3. Schematic representation of the polycrystalline gold nanoparticle, cut into four slices of thickness l along the z -direction.

The bulk absorption rate Γ is increased by a factor inversely proportional to the length scale L (slice thickness and/or particle dimensions). More precisely, in the direction perpendicular to the cut, $L=l$, whereas along the two parallel directions, $L=2R$.

S8. Depolarization ratio of grafted AuNPs with an analytical model in the quasi-static approximation

In the quasi-static approximation, where the wavelength of the incident plane wave is large compared to the nanoparticle dimensions, the retardation effects of the wave inside the particle can be neglected. It can be shown that the polarization inside a spheroid is then homogeneous and proportional to the incident electric field through:

$$\mathbf{P} = \frac{\bar{\bar{\alpha}}(\omega)}{V} \mathbf{E}_0$$

where the tensorial polarizability $\bar{\bar{\alpha}}(\omega)$ is diagonal inside the principal-axes frame of the spheroid:

$$\bar{\bar{\alpha}}(\omega) = \begin{bmatrix} \alpha_x & 0 & 0 \\ 0 & \alpha_y & 0 \\ 0 & 0 & \alpha_z \end{bmatrix}$$

Each diagonal term can be written as:

$$\alpha_i = V\epsilon_0 \frac{\epsilon_B \Delta\epsilon_i}{\epsilon_B + L_i \Delta\epsilon_i}, i = x, y, z \quad (1)$$

where $\Delta\epsilon_i = \epsilon_i(\omega) - \epsilon_B$ and L_i is the depolarization factor, which depends on the shape of the particle. Notice the dependency of the gold dielectric constant $\epsilon_i(\omega)$ on the direction $i = x, y, z$, necessary to describe the NP's polycrystallinity.

We will consider spheroids for which the symmetry axis is the z -axis. If b is the length of the semi-major axis and a the length of the semi-minor axis, the L_z factors are given Table S2.⁵

Table S2. Depolarization factors of a spheroid of semi-major axis length b and two identical semi-minor axis lengths a .

$r = b/a$	$r > 1$ (<i>prolate</i>)	$r < 1$ (<i>oblate</i>)
e	$\sqrt{1 - 1/r^2}$	$\sqrt{1 - r^2}$
L_z	$\frac{1 - e^2}{2e^3} \left(\ln \left(\frac{1 + e}{1 - e} \right) - 2e \right)$	$1 - \frac{g(e)}{e^2} \left(\frac{\pi}{2} - \text{atan}(g(e)) \right) + g(e)^2,$ $g(e) = \frac{\sqrt{1 - e^2}}{e}$

whereas $L_x = L_y = (1 - L_z)/2$.

The expression (1) can be generalized to a core-shell spheroid. With unchanged notations for the gold spheroidal core and considering the external shape of the shell (dielectric constant ϵ_1) with the same symmetry axis z , semi-major and semi-minor axis lengths respectively b' and a' , the polarizability components are:⁵

$$\alpha_i = V\epsilon_0 \frac{(\epsilon_1 - \epsilon_B)[\epsilon_1 + \Delta\epsilon_1(L_i^c - fL_i)] + f\epsilon_1\Delta\epsilon_1}{[\epsilon_1 + \Delta\epsilon_1(L_i^c - fL_i)][\epsilon_B + (\epsilon_1 - \epsilon_B)L_i] + fL_i\epsilon_1\Delta\epsilon_1}$$

with:

$$f = \frac{a^2b}{a'^2b'}$$

and:

$$\Delta\epsilon_1 = \epsilon_i(\omega) - \epsilon_1$$

The depolarization factors L_i and L_i^c have the same expression as in Table S2.

Finally, after averaging the AuNP orientation, the depolarization ratio $\rho(\omega) = I_{vh}(\omega)/I_{vv}(\omega)$ is:⁶

$$\rho(\omega) = 12 \frac{|\alpha_x + \alpha_y - 2\alpha_z|^2 + 3|\alpha_x - \alpha_y|^2}{5|\alpha_x + \alpha_y + \alpha_z|^2 + |\alpha_x + \alpha_y - 2\alpha_z|^2}$$

As an illustration, figure S4a shows the evolution of the maximum depolarization ratio ρ (occurring for a wavelength of about 532 nm) of a coreshell nanoparticle with spherical gold core and spheroidal shell with different refractive indexes n_{graft} . The value $a+b' = 25$ nm is kept constant while b' is varied from 0 nm to 25 nm. The polycrystallinity order is fixed to $n=2$, the cut plane being perpendicular to the NP revolution axis. The depolarization ratio is minimal for a spherical shell. Figure S4b shows the ratio $\rho^* = \rho(532 \text{ nm})/\rho(632 \text{ nm})$ as a function of b' , for different values of the shell refractive indexes. In order to obtain $\rho^* < 1$, the NP must be oblate, with a minimum value for b' decreasing with n_{graft} .

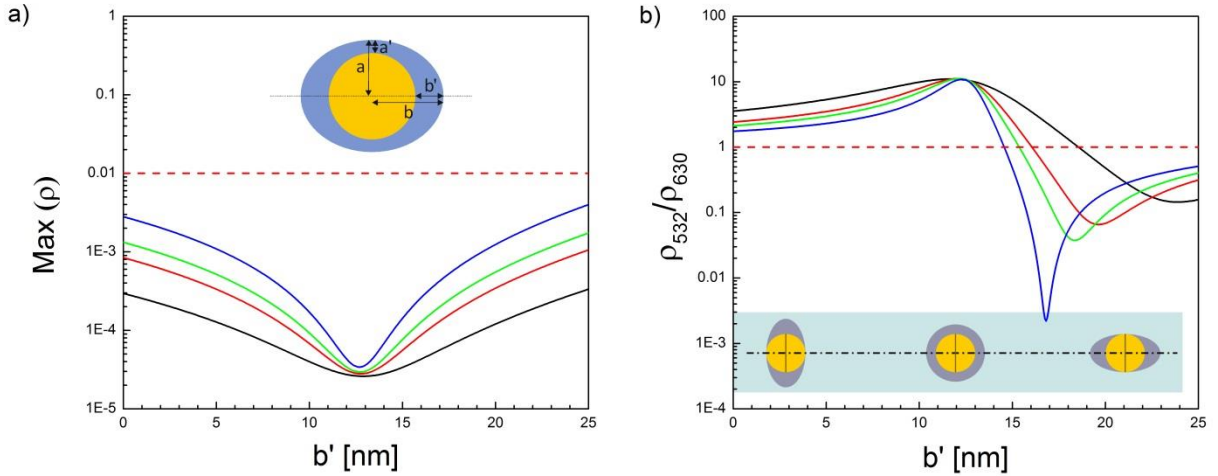


Figure S4. a) Depolarization ratio ρ for spherical gold cores as a function of the coating thickness and anisotropy along the particle long axis; b) ratio $\rho^* = \rho(532 \text{ nm})/\rho(632 \text{ nm})$. Black: $n_{\text{graft}}=1.40$, red: $n_{\text{graft}}=1.46$ (PEG), green: $n_{\text{graft}}=1.50$ (citrate), blue: $n_{\text{graft}}=1.60$ (DNA).

Table S3. Dimensions of the soft shell around the gold core for capturing the experimental data for D_{\perp}^r and D^t .

	p	a [nm]	b [nm]	κ
Au-citrate	1.3	22.01	28.6	2.95
Au-PEG₁₆	1.2	25.7	30.8	2.35
Au-PEG₄₅	1.2	29.5	35.4	1.85
Au-PEG₁₀₇	1.2	34.7	41.6	1.33
Au-PEG₁₀₇-COOH	1.2	34.9	41.9	1.55
Au-DNA_{T10}	1.1	31.0	34.1	1.95
Au-DNA_{T40}	1.1	35.0	38.5	1.55

S9. Perrin's equations⁷

$$D_{\perp}^r = \frac{k_B T}{6\eta V_{\text{hydro}} g_{\perp}}$$

$$g_{\perp} = \frac{2(p^4 - 1)}{3p[(2p^2 - 1)S - p]}$$

$$S_{\text{prolate}} = \frac{1}{\sqrt{p^2 - 1}} \ln \left[p + \sqrt{p^2 - 1} \right]$$

$$D^t = \frac{k_B T S_{\text{prolate}}}{6\pi\eta b}$$

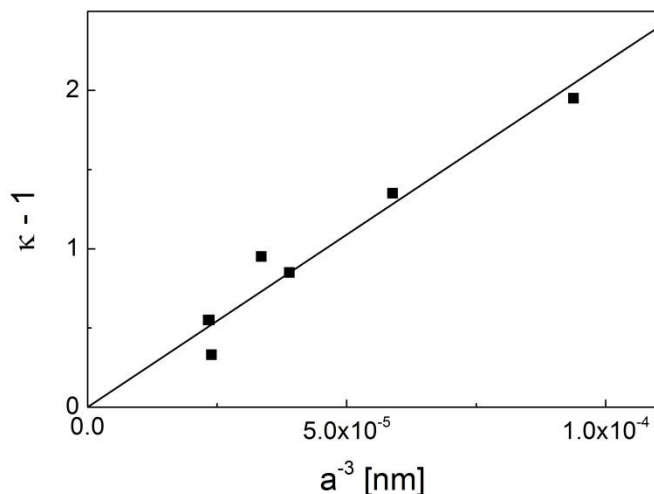


Fig. S5. The proportionality factor κ (black)= V_h/V_0 (V_h and V_0 denote the hydrodynamic and the geometrical volume) vs. $1/a^3$ for different grafts; κ approaches 1 at large a , and therefore $V_h = V_0$.

REFERENCES

1. Ziegler, C.; Eychmuller, A. *J Phys Chem C* **2011**, 115, 4502-4506.
2. Hanauer, M.; Pierrat, S.; Zins, I.; Lotz, A.; Sonnichsen, C. *Nano Lett* **2007**, 7, 2881-2885.
3. Martin, O. J. F.; Piller, N. B. *Phys Rev E* **1998**, 58, 3909-3915.
4. Berciaud, S.; Cognet, L.; Tamarat, P.; Lounis, B. *Nano Lett* **2005**, 5, 515-518.
5. Bohren, C.F., Huffman, D.R. *Absorption and Scattering of light by small particles*; Wiley-VCH: Weinheim, 1998.
6. Degiorgio, V.; Piazza, R.; Bellini, T.; Visca, M. *Adv Colloid Interfac* **1994**, 48, 61-91.
7. Kuipers, B. W. M.; van de Ven, M. C. A.; Baars, R. J.; Philipse, A. P. *J PhysCondens Mat* **2012**, 24, 545101.